Regulation and Rehabilitation of Hindlimb Gait Based on CPG in Rats with Spinal Cord Injury

Wei Shao
Nantong University
Xiaoyan Shen (xiaoyansho@ntu.edu.cn)
Nantong University
Zhiling Li
Nantong University
Qianqian Li
Nantong University
Yan Wu
Nantong University
Xiongjie Lou
Nantong University

Research

Keywords: CPG, One-port electrode, FES, Bioelectrical impedance measurement, Gait feedback and control

Posted Date: May 4th, 2021

DOI: https://doi.org/10.21203/rs.3.rs-432532/v1

Abstract

Background: To reconstruct hindlimb gait movement in patients with spinal cord injury(SCI), a spinal stimulator using a one-port electrode is proposed to regulate bilateral hindlimb movements in rats. Functional electrical stimulation(FES) of rats with spinal cord injury(SCI) was performed, considering the central pattern generator(CPG) in the spinal cord as the target.

Methods: Left hindlimb flexion and right hindlimb extension were achieved by stimulating the CPG site with a positive pulse, while negative pulse stimulation induced the opposite motions. Angle sensors were used to track and capture knee joint angle data, and the mapping relationship model between voltage amplitude and gait parameters was established. The hindlimbs were controlled using the reference angle. SCI rats were subjected to stimulation trained for 30 min each day for 28 days with a reference angle range of 96°-128°.

Results: Based on CPG site stimulation, the hindlimbs of rats were regulated between 96° and 128° with this system. On the 28^{th} day, a BBB score indicating. A 76% health level was achieved, while the SEP measurement results were close to the normal value.

Conclusion: Compared with traditional spinal stimulators, the proposed spinal stimulator has fewer electrodes and a simplified time sequence. The system realizes an improved gait feedback and decreased muscle fatigue. The results of rehabilitation training proved the recovery effect of the system on the hindlimb gait of SCI rats.

Background

SCI can cause different degrees of sensory, motor and autonomic nervous dysfunction, which seriously affects the normal life of patients [1]. According to the World Health Organization (WTO), at least 250,000 patients suffer from spinal cord injury each year, and the SCI patients in the world present an upward trend [2, 3]. The treatment of SCI has become a hotspot of research in biological science.

To date, interventions to restore functional walking after SCI in humans have had limited success. To activate muscles and nerves in the neural networks in the spinal cord or in its periphery as well as to restore movement, one of the most promising techniques is functional electrical stimulation (FES)[4, 5]. Grégoire Courtine et al. used the stimulation of neuron targets to restore paralyzed hindlimb movement of monkeys with spinal cord hemisection. Following the study of the rat spinal cord FES model, they combined the spinal cord FES with body weight adjuvant therapy to restore the control of leg muscles in paralyzed patients over a period of many years[6, 7]. Peckham et al. successfully designed a 62-channel FES systemsto control hindlimb movement[8]. Holinski et al. performed FES on the spinal cord neural network of anesthetized cats. A microwire electrode array with eight Pt/Ir electrodes was used to achieve long-distance propulsive walking in anesthetized cats[9]. If FES uses muscle as the stimulation object, then different muscle groups need to be stimulated at different times. These muscles are prone to fatigue, and hence, the walking distances are limited[10]. If FES uses motor neurons as the stimulation object, then

a complex array of stimuli is often required. These stimulation systems require a large number of stimulation channels with a complex timing control. If the neural network can be used as the stimulus object, the number of stimulation electrodes can be effectively reduced and the time sequence can be simplified.

Central pattern generators(CPGs) are groups of neural networks, that generate rhythmic control output. In vertebrates, the basic motor function is generated by spinal CPGs. The autonomously generated signal can be combined with the control signal from the higher center to generate gait movement. In an experiment on rats, it was found that there were some specific CPG sites in the spinal cord. By stimulating these sites with certain pulse signals, an alternating movement of the hind limbs can be achieved with fewer electrodes. Gait rehabilitation training using an activated neural network can recover gait movement in a way that is closer to the physiological state and with fewer electrodes [11, 12]. Therefore, the establishment of a gait regulation system with a one-port stimulation electrode based on CPG is proposed.

In this study, we identified several CPG sites that control the alternating movement of bilateral hindlimbs. However, only one site on each side caused an alternating motion mode triggered by the polarity reversal of the stimulus signal. The right CPG site was stimulated by a positive pulse inducing a right hind limb extension and left hindlimb flexion, while a negative pulse stimulation gave the opposite result. Consequently, a complete gait motion can be achieved by the stimulation of positive and negative pulses[13].

The gait control system uses special unilateral CPG as the target for stimulation and automatic control. The pulse width of the signal was 200μs, the interval was 30ms, and the amplitude was adjustable. To establish a model of the stimulating signal parameters and angles [14, 15], the parameters of the stimulation signals are automatically adjusted according to the stride length and the frequency of training. Using the model, Automatic training of the bilateral hindlimbs of rats with spinal cord injury(SCI) was performed. To ensure that the electrodes contact, an impedance measurement part was added to determine whether the electrode contacted the epidermis and was oxidized.

Results

Amplitude - Angle model validation

The stimulator was applied to the hindlimb gait control in rats. The reference frames(106–127°) were set up to verify the correlation between the actual angle and the reference frame. Figure 1 shows a comparison between the angle after closed-loop feedback control and the angle of the reference system. The red line represents the actual knee joint angle data of the rats. It can be observed that the actual angle data is always near the reference frame. In the amplitude control stage, the maximum error is 2°. It has been proven that the system can stabilize the actual gait of rats in the reference frame and effectively control the hindlimb gait of rats.

BBB scale

Figure 2 shows the comparison of BBB scores between SCI + ES and SCI rats. SCI + ES group could move the hind limb joints slightly, while SCI group did not observe the slight movement of the hind limb joints. BBB scores of SCI on 21d and 28d were 8.67 ± 0.94 and 10.67 ± 0.47 respectively, and those of SCI + ES group were 12.34 ± 2.62 and 15.33 ± 1.41 respectively. Compared with SCI group, SCI + ES group showed significant changes in behavioral function recovery within 4 weeks. This result indicates that the stimulation training with this system can make SCI rats recovery better.

SEP data analysis

The data of SEP was analyzed to enhance the contrast of the Intact rats. Figure 3 shows the comparison of p-wave latency of four SCI + ES and SCI with the intact rats in each group. The mean values of SCI + ES differed 2.4ms against the intact rats and the mean values of SCI differed 9.94ms against the intact rats. Figure 4 shows the comparison of N-wave latency of four SCI + ES and SCI with the intact rats in each group. The mean values of both rats differed 2ms and 5.93ms against the intact after 28 days. Figure 5 shows the comparison of N-wave amplitude of four SCI + ES and SCI with the intact rats in each group. The mean values of both rats differed3.27mV and 5.31mV against the intact after 28 days. Figure 6 shows the comparison of N waves amplitude of four SCI + ES and SCI with the intact rats in each group. The mean values of both rats differed 3.22mV and 5.2mV against the intact 28 days later. Stimulation training with this system has obvious effect on the recovery of rat hind limb.

Discussion

A traditional spinal cord stimulator has a relatively complex timing sequence with a large number of stimulation sites and stimulation channels. Although it can help restore limb movement, to a certain extent, its high cost limits the development of spinal cord stimulators.

The purpose of the proposed system is to establish a stimulus system using only a one-port electrode. It combines a microcontroller, a sensor, and an host computer, and it has advantages including a low cost and a simple timing sequence. It automatically adjusts the hindlimb movement of rats according to the preset angle of the knee joint. Based on the CPG target, rats can be induced to alternate hindlimb motion by reversing the polarity of the stimulus signal. The reference motion angle function was derived according to the actual motion angle of the hindlimb. The amplitude of the signal was regulated by a DAC at 1.289–2.255 V at a frequency of 10 Hz, and the step size was 0.161 V based on the reference motion angle function, which was used to realize the automatic control of the stride length and frequency of bilateral hindlimbs of rats.

Stimulation of a single CPG site can effectively reduce muscle fatigue in rats. Compared with the actual gait movement of rats, relatively accurate regulation of a certain range of gait at one site of CPG stimulation can be achieved through feedback. Finally, the impedance detection of the stimulation site was increased to prevent deviation of the electrode during stimulation and improve the safety and robustness of the stimulation. The test showed that the range of the knee angle was 60°–140° when the hindlimbs of intact rats moved while normal walking. Based on results from different SCI rats, the CPG

functional electric stimulation system could achieve an adjustable range of knee angles between 90° and 128° by stimulation with a one-port electrode, which was only slightly different from normal walking.

According to the analysis of the BBB score and SEP data, the rats' hindlimb motor function recovered quickly after stimulation training with the stimulus system. Although the gait movement existing before the spinal cord injury could not be completely recovered, the gait rehabilitation effect was significant compared with that of rats without stimulation training. Thus, the proposed system can be effectively applied to the rehabilitation training of hindlimb gait in rats with SCI for subsequent implementation in clinical rehabilitation training.

Conclusion

The stimulation system achieved gait regulation and rehabilitation training in SCI rats using a one-port electrode. One-port stimulation training in SCI rats confirmed a positive effect on hindlimb recovery. This is of great significance for the study of SCI treatments and low-cost stimulation devices.

To increase the precision of closed-loop control, a self-learning algorithm can be added based on the original model. This modified model can optimize the regulated pulse amplitude parameters iteratively to achieve the desired angular motion. In addition, the measurement of the angle can be expanded from a one-dimensional angle to a three-dimensional angle to reduce the error of closed-loop control.

Methods

System design

The general framework for the hindlimb gait control system based on CPG for rats with SCI is shown in Fig. 7. The initial value of the stimulator is provided according to the stride length and frequency set by the host computer. The stimulator provides positive and negative pulse signals to the one-port electrode, which is connected with the CPG site, this induces bilateral gait movement of the hindlimbs of the rats. The unilateral hind limb gait of the rats was measured by detecting the knee joint angle of the hindlimb of rats, and the data were displayed on the screen. In line with the model of stimulating signal parameters for stride length and frequency, when the knee joint angle is extremely large or small, the pulse amplitude is reduced or increased. When the step frequency is extremely high or low, the stimulation signal period is lengthened or shortened resulting in automatic control of hindlimb movement in rats.

The stimulator utilizes an STM32F103 and communicates with the host computer by ZigBee[16]. STM32F103 with a voltage output digital-analog converter (DAC). The 12-bit digital input DAC, configured by the system, uses two timers to control the voltage amplitude of output signal. The voltage follower and subtraction circuit, composed of two LM358Ns, generate positive and negative pulse signals to stimulate the CPG site. To obtain the relationship model between the gait angle data and signal parameters, the stimulator is equipped with buttons to control the signal parameters and record angle data. The knee joint angle information was obtained using two JY901 sensors, and the data transmitted to the stimulator via a

serial port. The JY901 sensor, integrated with high-precision gyroscope, derives the motion posture in real time[17]. In a dynamic environment, the measurement angle error is only 0.1°, which meets the requirements of knee joint angle measurement. The stimulation electrode is either in contact with the epidermis or is oxidized when stimulating the CPG site; thus the impedance measurement part is added to the system. As the impedance measurement and stimulation are both required at the same key CPG site, a single tungsten wire electrode is used as an impedance measurement probe and a stimulation electrode to achieve a dual-purpose function. In the circuit design, a relay is used to make or break the connection between the impedance measurement circuit and the stimulation circuit and thus prevent the influence of the stimulation circuit on impedance measurement[18]. An AD5933 was used as the impedance measurement chip, and a two-point calibration method was used to measure impedance. The starting frequency was 29,000Hz, the number of scanning points was 16, and the frequency increment was 62.5Hz. Each frequency point was repeated four times to obtain an average value of the real and imaginary parts, and thus obtain the corresponding amplitude and phase. The calculated impedance value displayed on the screen[19]. According to the range of the spinal cord impedance, the calibration resistance was set to $1K\Omega$[20].

The operation of the system is divided into two parts. First, confirming that the impedance is within the set threshold, the system shows the green light and selects the initial stimulus signal according to the preset stride and frequency. Second, a set of gait angle information is detected. The hindlimb movement is automatically adjusted according to the mapping model of the signal and angle. In the first part, if the impedance is not within the set range, a red light prompts the user to check the problem. In the second part, when the automatic adjustment of the hind limb fails to reach the reasonable range of the reference frame, the stimulator is stopped, indicating that the rats may have muscle fatigue.

Experiment

All experimental programs involved in animal use in this study were approved by the animal care and use Committee of Nantong University. We guarantee that all applicable institutions and government regulations on ethical use of animals are observed in the course of this study.

The experiment serves two purposes. One is to establish the model of the relationship between the knee joint angle of the hind limb and positive and negative voltage pulse amplitude. The other is to verify the effect of stimulator on gait function recovery. The way is to stimulate SCI rats to carry out gait training under the pre-set stride length and frequency.

Subjects

Sprague Dawley (SD) rats, weighing about 250g, of either sex, were used in the experiment. In the experiment, 10% chloral hydrate was injected intraperitoneally. After anesthesia and pre-operative skin preparation, the skin surface of the rats was disinfected with 75% alcohol and the epidermis was cut off. The segment lamina of T12-T13 vertebrae in rats were removed to expose the spinal cord. The T9 segment of spinal cord was hammered. The hammer with a diameter of 2.5mm and weighing 10g is used to hammer the T9 segment at a height of 6.25mm.

The locations of the right CPG site in the lumbosacral spinal cord was described as the position in the corresponding vertebral segment, denoted as *(x, y, z)*. The mediolateral direction X was normalized by D/2, the dorsoventral direction Y was normalized by D, and the rostrocaudal direction Z was normalized by L. According to the coordinates of intact rats: the right CPG site is determined as *(X, Y, Z) = (0.377 ± 0.196, 0.619 ± 0.019, 0.780 ± 0.143)*. The right CPG site was stimulated by positive pulse to induce right hind limb extension and left hindlimb flexion. Negative pulse stimulation of the right CPG site induced the right hind limb flexion and left hindlimb extension. Tungsten wire electrode was implanted at this site and fixed with dental cement. Finally, the wound was sutured and anti-inflammatory drugs were injected into the experimental rats and the experiment was carried out three days later.

Amplitude-angle model

Three rat subjects with fixed electrodes were used to build the stimulation model. The gait is derived by measuring the knee joint angle of the unilateral hindlimb of SD rats. The sensor position and knee joint angle θ are shown in Fig. 8. The correlation between the stimulus signal voltage amplitude and gait angle data is converted into a mapping relationship. The CPG site was stimulated by pressing the button to change the voltage amplitude of the stimulus signal, and the knee joint angle of the unilateral hindlimb was measured to establish the knee joint angle and signal parameter model[21–23].

During the stimulation experiment on SCI rats, it was observed that by changing the amplitude of stimulation signal in 0.161 V steps, the movement of hindlimbs can be regulated more smoothly and accurately. When the amplitude of the stimulus signal is too weak then no movement can be observed. When the amplitude is extremely strong, precise regulation cannot be achieved. For voltage amplitudes between 1.289–2.255V, the gait changes of the hindlimbs of rats is clearly observed, which is in accordance with the closed-loop control of the system.

In order to get the relationship between amplitude parameters of stimulus signal and knee joint angle, the method of separating variables is used[24]. The mapping between the different voltage amplitudes and knee joint angles are shown in the Fig. 9, Fig. 10. When the CPG of anesthetized SCI rats was not stimulated, the knee joint angle of different rats was generally stable at between 118 ° and 122 °. In Fig. 9, the positive pulse amplitude is constant at 1.289 V, and the negative voltage changes from − 1.289 V to -2.255 V in step of 0.161 V. Table 1 shows the minimum knee joint angle of each rat and the mean of the three rats. In Fig. 10, the negative pulse amplitude constant at minus 2.255 V, and the positive voltage changes from + 1.289 V to + 2.255 V in step of 0.161V. Table 2 shows the maximum knee joint angle of each rat and the mean of the three rats. The experimental analysis showes that the positive and negative pulse amplitudes have different effects on the angle change.

Table 1
Minimum and mean values of the knee joint angles of the three rats with the increase of negative voltage

□□(V)	-1.289	-1.450	-1.611	-1.772	-1.933	-2.094	-2.255
□□							
□	110.41°	107.32°	106.45°	104.60°	101.28°	98.63°	97.64°
□	109.52°	107.61°	106.69°	104.39°	102.43°	99.87°	97.53°
□	109.28°	108.56°	105.06°	102.87°	99.23°	97.86.°	96.37°
Mean	109.73°	107.83°	106.06°	103.95°	100.98°	98.78°	97.18°

Table 2
The maximum and mean values of the knee joint angles of the three rats with the increase of positive voltage

□□(V)	+1.289	+1.450	+1.611	+1.772	+1.933	+2.094	+2.255
□□							
□	126.32°	126.85°	128.13°	129.94°	130.9°	131.32°	131.61°
□	127.13°	127.76°	128.82°	129.62°	130.35°	130.93°	131.42°
□	126.95°	128.19°	129.35°	129.54°	130.25°	130.75°	131.17°
Mean	126.8°	127.6°	128.8°	129.7°	130.5°	131.0°	131.4°

The experimental results show that the positive and negative pulse amplitudes have different effects on the angle variation. As shown in Fig. 11, β represents the angle variation range of the knee joint of rats, *Step* represents the amplitude of the pulse signal to control the Step size, α represents the initial angle of rats without stimulation, θ_1 represents the angle variation range of positive impulse stimulation, and θ_2 represents the angle variation range of negative impulse stimulation. The relationship between parameters is shown as follows. The relationship model between amplitude and angle is established.

The variation range of knee joint angle $\beta \in$ (96°~132°),

Step size of amplitude regulation *Step* = 0.161V,

The initial angle $\alpha \in$ (118°~122°),

θ_1 is the control range of positive pulse change,

θ_2 is the control range of negative pulse change,

Under stimulation by a positive pulse signal, the right hindlimb is extended, with knee joint θ_1 was approximately 1 °. Under stimulation by a negative pulse signal, the right hindlimb is flexed, with knee joint

θ_2 was approximately 2 °. The angle of the knee joint gradually returned to normal when the stimulation was removed.Relationship model between amplitude and knee joint angle is is shown in Eq. 2 − 1 and 2–2:

$\theta_1 = \alpha + \gamma_1 \pm Nstep$ (γ_1 is the angle of extension of hind limbs) (2 − 1)

$\theta_2 = \beta + \gamma_2 \pm 2Nstep$ (γ_2 is the angle of flexion of the hind limbs) (2–2)

The results showed that the stimulation effect of negative pulse on CPG site was more obvious[25], and the range of positive and negative pulse signals between 1.289 and 2.255V maintained the range of knee joint angle between 96° and 132° when the CPG site was stimulated.

The reference angle of the rat hind limb movement automatically controlled by the system was set reasonably according to the actual knee angle. The actual angle was obtained by stimulating the CPG of SCI rats with different stimulus signals. At the same time, the sampling frequency was set to 10Hz to enable comparition of the actual angle and the reference angle [26]. The knee joint angle of SCI rats was automatically adjusted according to the reference angle set by the voltage amplitude and interval time. The reference angle is expressed as piecewise functions namely positive pulse stimulation, negative pulse stimulation, and stimulus interval. A reasonable reference angle range was set according to the actual movement angle range of the CPG stimulation. There are many types of knee joint angle changes, as shown in Table 3 and Table 4. These show knee joint angle forms of reference gait change, which correspond to positive and negative pulse stimulation, respectively, and the corresponding reference frame function is synthesized. The lowest stimulation period of the system is 2.1 s(There are 20 positive pulse waveforms with a pulse width of 200us and 20 negative pulse waveforms with a pulse width of 200us. The pulse interval is 30ms, and the minimum interval of positive and negative pulse is 0.9s).

Table 3
The coordinate of positive pulse reference system is taken

t/s	kT + 0.8	kT + 0.9	kT + 1	kT + 1.1	kT + 1.2	kT + 1.3	kT + 1.4	kT + 1.5	kT + 1.6	kT + 1.7
106/127	120	121	123	126	127	126	122	122	121	119
102/129	118	122	125	127	129	128	121	120	119	121
96/132	119	121	123	126	132	129	127	122	121	120

Table 4
coordinates of negative pulse reference system

t /s	kT + 1.7S + T′	kT + 1.7S + T′+0.1	kT + 1.7S + T′+0.2	kT + 1.7S + T′+0.3	kT + 1.7S + T′+0.4	kT + 1.7S + T′+0.5	kT + 1.7S + T′+0.6	kT + 1.7S + T′+0.7	kT + 1.7S + T′+0.8	kT + 1.7S + T′+0.9
106/127	120	118	107	107	106	107	108	110	115	120
102/129	122	115	108	104	102	104	108	116	118	119
96/132	121	118	110	101	96	99	102	115	117	118

The reference frame is fitted in the first period range. When entering the gait control range of the second period, the collection time of the system is set as the initial value, which is equivalent to continuing to cycle the control with the reference angle of the first period.

In the first cycle (K = 0), the fitting function of knee joint angle under positive and negative pulse stimulation is shown in Eq. 2–3.

$$\lambda_2 = f(x) = a_1 * \sin(b_1 * x + c_1) + a_2 * \sin(b_2 * x + c_2) + a_3 * \sin(b_3 * x + c_3) \quad (2-3)$$

When the reference frame of 106 ~ 127° is selected, the positive pulse fitting function is shown in Fig. 12.

$a_1 = 850.4, b_1 = 2.29, c_1 = 0.62, a_2 = 725.7, b_2 = 2.48, c_2 = 3.68, a_3 = 2.48, b_3 = 11.42, c_3 = 3.37.$

The negative pulse fitting function is shown in Fig. 13.

$a_1 = 122.9, b_1 = 1.67, c_1 = 0.82, a_2 = 42.18, b_2 = 6.8, c_2 = 1.62, a_3 = 15.6, b_3 = 8.09, c_3 = 4.05.$

In the time interval between positive and negative pulses, the fitting function is shown in Eq. 2–4.

$$y \in [118, 122], x \in [kT + 1.7, kT + 1.7 + T'] \quad (2-4)$$

Equation 2–4 indicates that in the interval time, the angles from 118° to 122° meet the regulation requirements. These functions are divided into three segments, and combined into a reference angle system to regulate the hindlimb gait of rats.

The positive pulse reference frame coefficient at 102 ~ 129°:

$a_1 = 779.3, b_1 = 2.16, c_1 = 0.3, a_2 = 655.4, b_2 = 2.35, c_2 = 3.32, a_3 = 2.25, b_3 = 13.4, c_3 = 2.08.$

The negtive pulse reference frame coefficient at 102 ~ 129°:

$a_1 = 263.9, b_1 = 2.24, c_1 = 0.74, a_2 = 161.8, b_2 = 3.23, c_2 = 3.5, a_3 = 0.66, b_3 = 18.84, c_3 = 1.23.$

The positive pulse reference frame coefficient at 96 ~ 132°:

$a_1 = 367.8, b_1 = 2.61, c_1 = 0.38, a_2 = 242, b_2 = 3.28, c_2 = 3.21, a_3 = 5.29, b_3 = 10.64, c_3 = 3.08.$

The negtive pulse reference frame coefficient at 96 ~ 132°:

$a_1 = 136.5, b_1 = 2.01, c_1 = 0.68, a_2 = 46.35, b_2 = 5.80, c_2 = 2.13, a_3 = 6.11, b_3 = 8.18, c_3 = 3.96.$

In the closed-loop control of the system, to ensure that the sampled knee joint angle does not deviate from the reference angle, reference points are set for the actual angle information, which are the starting position and the minimum point in each cycle, as shown in Fig. 14. The initial calibration point is correctly set when the angle return value is stable within 118° to 122° for a period of time. The minimum calibration point within a time period is the minimum value resulting from the angle data collected within the time period of the signal. The sampling period of the sensor is set as 0.025s to ensure the correctness of the sampling point.

Gait training

To evaluate the recovery of hind limb of rats after training, the rats used in the experiment are divided into two models: spinal cord injury rats (SCI), spinal cord injury rats and stimulation training rats (SCI + ES).

SCI + ES rats were trained three days after spinal cord injury, the knee joint reference angle in the range of 96°to128°was set in advance. SCI + ES rats received training five times a week (30 minutes each time) for four weeks to recover the involuntary hind limb movement ability. Rats in SCI + ES group were compared with rats in SCI group to judge the recovery of rats' hind limbs.

Data recording

Two gait angle sensors are calibrated in the same environment, and the data is sent to the processor through serial port. The communication protocol is shown in Table 5. The system sets the angle output rate to 40Hz and the serial port baud rate to 9600bps.

Table 5
JY901 angle Transport Protocol table

Start bit	The X-axis Angle	The Y-axis Angle	The Z-axis Angle	Temperature	Checksum
0x55 0x53	DegxL + DegxH	DegyL + DegyH	DegzL + DegzH	TL + TH	SUM

According to Table 5, the angle of y-axis is obtained as follows:

Deg_y=((DegyH<<8)| DegyL)/32768*180°

The processor receives the real-time data of the y-axis direction of the two sensors and analyzes the real-time data of the knee joint angle of the rat.

Basso, Beattie and Bresnahan (BBB) motor abilities were scored on days 3, 5, 7, 10, 14, 21 and 28 after surgery in SCI and SCI + ES rats to evaluate hindlimb motor functions. In the BBB tests using two non-experimenters, the rats were allowed to move freely and the motor function of both hindlimbs was

recorded with the highest score on the BBB score, being 21. The higher the score, the better the motor function. Experimental animal groups were also used for independent evaluation (double-blind method), and the average values were recorded [27, 28].

Somatosensory evoked potentials(SEP) was recorded on days 7, 14, 21 and 28. When SEP was recorded, the hindlimb ankle was stimulated by the stimulation signal generated by Keypoint Table Electromyography. The hindlimb somatosensory triggered signal goes to the brain and is monitored by the electrode implanted in the head [29]. The stimulation electrode was triggered by an electric pulse of 4mA, pulse width of 0.1ms, frequency of 3Hz, and repeated 200 times. The stimulation intensity was set to make the toes of the hind limbs twitch slightly. The latency of the applied potential and wave amplitude is used (peak downward is P, upward is N) to judge the recovery of hindlimbs. The latency period reflects the conduction distance, velocity, and synaptic delay time of the action potential with a shorter latency period, indicating better recovery. The amplitude (uV) reflects the number of synchronous firing neurons with higher amplitude, indicating better recovery.

The BBB score and SEP data in SCI + ES rats were analyzed, and compared with SCI rats to judge the recovery of lower limb gait.

Gait closed-loop control

The closed-loop control of gait mainly regulates the stride length and frequency, which are divided into angle data processing and DAC amplitude modulation. The knee joint angle information λ_1 collected by the system every second was compared with the preset reference frame angle λ_2. S represents the minimum step size of DAC parameter regulation. When stimulated, the angle of the hindlimb was changed to θ_1 with positive pulse stimulation and θ_2 with negative pulse stimulation. In stride regulation, the stride amplitude is related to the pulse amplitude. In positive pulse stimulation, $n=|\lambda_1-\lambda_2|/\theta_1$, in negative pulse stimulation, $n=|\lambda_1-\lambda_2|/\theta_2$. In step frequency regulation, the step frequency is related to the interval between the positive and negative pulses. The amplitude of stimulus signal tends to 0, and λ_1 and λ_2 are close to each other, n is approximately 0 (n is the number of times to adjust the parameter s, round the integer value). $S = 0.161V$, $\theta_1 = 1°$, $\theta_2 = 2°$ are obtained. The closed-loop control process is shown in Fig. 15.

In the process of positive pulse stimulation, assuming that the acquisition angle at t_1 is λ_1, and the reference frame angle corresponding to t_1 is $\lambda_2 = f(t_1)$, $\lambda_2 > \lambda_1$, then the number of increasing steps is $n=(\lambda_2-\lambda_1)/1$. If $\lambda_2 < \lambda_1$, then the number of step sizes reduced is $n=(\lambda_1-\lambda_2)/1$. In the process of negative pulse stimulation, the acquisition angle at t_2 is assumed to be λ_1', and the angle coordinate of t_2 reference frame is $\lambda_2' = f(t_2)$, $\lambda_2' > \lambda_1'$, the number of increasing steps is $n=(\lambda_2'-\lambda_1')/2$. If $\lambda_2' < \lambda_1'$, the number of steps reduced is $n=(\lambda_1'-\lambda_2')/2$ (t is the sampling interval time of reference frame angle).

Assessment Methods

The methods for evaluating the recovery of motor function combines behavior, kinesiology and physiology. Initial assessment for movement characteristics was used BBB scales [30]. EMG, kinematics [31], grip strength [32] was conducted to precisely assess hindlimb function recovery ability. SEP [33–35] was used to detect the electrophysiological function of rats as a means to evaluate recovery of spinal pathways.

Abbreviations

SCI: Spinal cord injury; CPG: Central pattern generator; BBB: Basso, Beattie and Bresnahan; SEP: Somatosensory evoked potentials.

Declarations

Authors` contributions

SW prepared the manuscript, system design and all data analysis; SXY provided lab and writing guidance; LZL and WY looked for CPG sites in rats; LQQ and LXJ were responsible for PCB production.

Author details

[1]School of Information Science and Technology, Nantong University, Jiangsu, China

[2]Co-innovation Center of Neuroregeneration, Nantong University, Jiangsu, China

Declaration of Computing Interest

We declare that we do not have any commercial or associative interest that represents a conflict of interest in connection with the work submitted.

Acknowledgement

This work was supported by National Natural Science Foundation of China (61534003, 81371663) and Opening Project of State Key Laboratory of Bioelectronics in Southeast University. This work was also supported by the "Six talents peaks" Project (SWYY-116), the “226 Engineering” Research Project of Nantong Government.

Availability of data and materials

The datasets used or analysed during the current study are available from the corresponding author on reasonable request.

Consent for publication

Written informed consent for publication was obtained from all participants.

Ethics approval and consent to participate

Attached is the proof.

Funding

National Natural Science Foundation of China (61534003, 81371663) and Opening Project of State Key Laboratory of Bioelectronics in Southeast University.

References

1. Wesley Chay MD, Steven Kirshblum MD. Predicting Outcomes After Spinal Cord Injury[J]. Physical Medicine Rehabilitation Clinics of North America. 2020;31(3):331–43.
2. Chiu WT, Lin HC, Lam C, et al. Review paper: epidemiology of traumatic spinal cord injury: comparisons between developed and developing countries[J]. Asia-Pacific journal of public health /. Asia-Pacific Academic Consortium for Public Health. 2010;22(1):9–18.
3. Giagka V. Flexible active electrode arrays for epidural spinal cord stimulation[M]. University College London; 2015.
4. Ofner P, Muller-Putz GR. Using a Noninvasive Decoding Method to Classify Rhythmic Movement Imaginations of the Arm in Two Planes[J]. IEEE Trans Biomed Eng. 2015;62(3):972–81.
5. Boulenguez P, Vinay L. Strategies to restore motor functions after spinal cord injury[J]. Curr Opin Neurobiol. 2009;19:587–600.
6. Vand BR, Heutschi J, Barraud Q, et al. Restoring voluntary control of locomotion after paralyzing spinal cord injury[J]. Science. 2012;336(6085):1182–5.
7. Capogrosso M, Milekovic T, Borton D, et al. A brain-spine interface alleviating gait deficits after spinal cord injury in primates[J]. Nature. 2016;539(7628):284–8.
8. Kilgore KL, Peckham H, et al. An implanted upper extremity neuroprosthesis: A five patient follow-up [J]. Journal of Bone Joint Surgery. 1997;79(4):533–41.
9. Holinski BJ, Mazurek KA, Everaert DG, et al. Intraspinal microstimulation produces over-ground walking in anesthetized cats. J Neural Eng. 2016;13(5):056016.
10. Thrasher TA, Popovic MR. Functional electrical stimulation of walking: Function, exercise and rehabilitation[J]. Annales de readaptation et de medecine physique, 2008, 51(6):pp. 452–60.
11. Zheng Y, Hu X. Elicited upper limb motions through transcutaneous cervical spinal cord stimulation[J]. J Neural Eng. 2020;17(3):036001 (10pp).
12. B J D A, A F C.. A controller perspective on biological gait control: Reflexes and central pattern generators[J]. Annual Reviews in Control. 2019;48:392–400.
13. Shen X, Li Z, Ma L. Double-electrode electronic system for reconstructing gait motor function[P]. Australia, LU101751,2020.

14. Petrucci MN, Neuville RS, Afzal MF, et al. Neural Closed loop deep brain stimulation for freezing of Gait[J]. Brain Stimulation. 2020;13(5):1320–2.
15. Coste CA, Sijobert B, Froger J, et al. Preliminary developments towards closed-loop FES-assistance of posture and gait[J]. Ifac Papersonline. 2015;48(20):333–7.
16. Wadhwa LK, Deshpande RS, Priye V. Extended shortcut tree routing for ZigBee based wireless sensor network[J]. Ad Hoc Netw. 2016;37:295–300.
17. Liu R, Peng L, Tong L, et al. The Design of Wearable Wireless Inertial Measurement Unit for Body motion Capture System[C]. IEEE International Conference on Intelligence and Safety for Robotics. The Electrical Engineering and Automation Department, China University of Mining and Technology (Beijing), Beijing, CO, 100083, China.
18. Yin T, Chen X, Yin H. Research On Embedded Electrical Impedance Measurement System[J]. Proceedings of International Conference on Artificial Life and Robotics,2019,24:382–386.
19. Yusoff, Mhd MA. Development of an AD5933-based Impedance Meter Prototype for Impedimetric Sensor Applications[J]. Procedia Chem. 2016;20:56–9.
20. Patrick A, Cody JR, Eles, Carl F, Lagenaur, et al. Unique electrophysiological and impedance signatures between encapsulation types: An analysis of biological Utah array failure and benefit of a biomimetic coating in a rat model[J]. Biomaterials. 2018;161:117–28.
21. Duysens J. Arturo Forner-Cordero. A controller perspective on biological gait control: Reflexes and central pattern generators[J]. Annual Reviews in Control. 2019;48:392–400.
22. Chou chihhong, Tong W, et al. Automated functional electrical stimulation training system for upper-limb function recovery in poststroke patients[J]. 84: Medical Engineering & Physics; 2020. pp. 174–83.
23. Joucla Sébastien A, Matthieu L, Timothée, et al. Generation of Locomotor-Like Activity in the Isolated Rat Spinal Cord Using Intraspinal Electrical Microstimulation Driven by a Digital Neuromorphic CPG[J]. Frontiers in neuroscience,2016,10:67.
24. Joucla Sébastien A, Matthieu L, Timothée, et al. Generation of Locomotor-Like Activity in the Isolated Rat Spinal Cord Using Intraspinal Electrical Microstimulation Driven by a Digital Neuromorphic CPG,2016,10:67.
25. Coste CA, Sijobert B, Froger J, et al. Preliminary developments towards closed-loop FES-assistance of posture and gait[J]. Ifac Papersonline,2015,48(20):333–337.
26. Ichihara K, Ozarda Y, Barth JH, et al. A global multicenter study on reference values:1. Assessment of methods for derivation and comparison of reference intervals[J]. Clin Chim Acta. 2016;467:70–82.
27. Evans RM, Davies M. ScoreCentre. A computer program to assist with collection and calculation of BBB locomotor scale data[J]. J Neuro Methods. 2010;194(1):102–7.
28. Lee CS, Leong KW. Advances in microphysiological blood-brain barrier (BBB) models towards drug delivery[J]. Curr Opin Biotechnol. 2020;66:78–87.
29. Pereira P. Leote, et al. Stimulus waveform determines the characteristics of sensory nerve action potentials[J]. Clinical Neurophysiology Shannon. 2016;127(3):1879–85.

30. Basso DM, Beattie MS, Bresnahan JC. Graded histological and locomotor outcomes after spinal cord contusion using the NYU weight-drop device versus transection. Exp Neurol. 1996;139(2):244–56.
31. Islam R, Cuellar CA, Felmlee B, et al. Multifactorial motor behavior assessment for real-time evaluation of emerging therapeutics to treat neurologic impairments[J]. Sci Rep. 2019;9(1):16503.
32. Alam M, Garcia-Alias G, Shah PK, et al. Evaluation of optimal electrode configurations for epidural spinal cord stimulation in cervical spinal cord injured rats[J]. Journal of Neurosci Methods. 2015;247:50–7.
33. Cheng XH, Zhang L, Fu J. Somatosensory evoked potential changes and decompression timing for spinal cord function recovery and evoked potentials in rats with spinal cord injury[J]. Brain Research Bulletin,2019,146:7–11.
34. Agrawal G, Kerr C, Thakor NV, et al. Characterization of graded multicenter animal spinal cord injury study contusion spinal cord injury using somatosensory-evoked potentials[J]. Spine,2010,35(11):1122–7.
35. Zhou X, Zhang B, Qiao K, et al. Central nervous system impairment detected by somatosensory evoked potentials in patients with Charcot-Marie-Tooth disease type 1A[J]. Journal of Clinical Neuroence,2020,79:191–196.

Figures

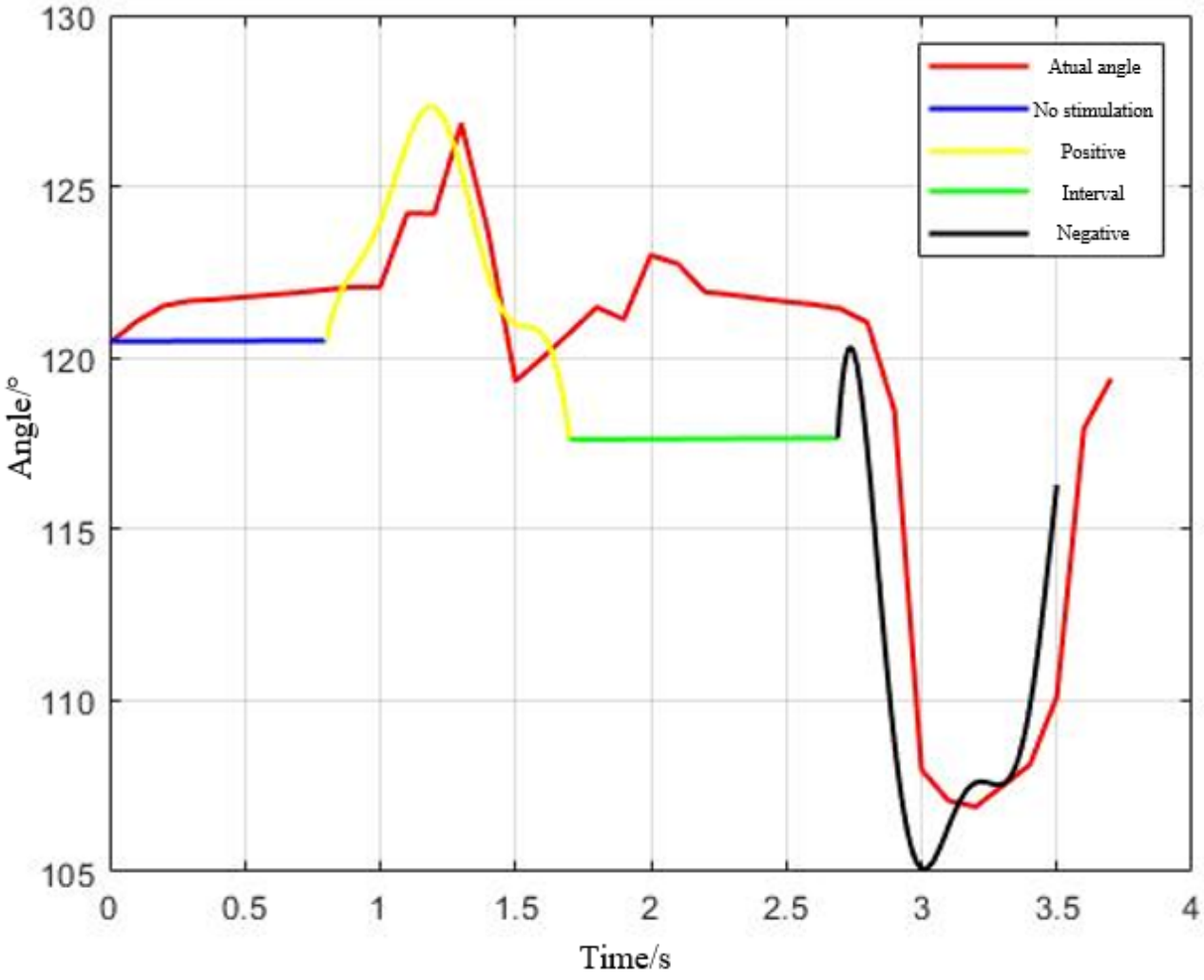

Figure 1

Comparison diagram of closed-loop control knee joint angle with reference frame

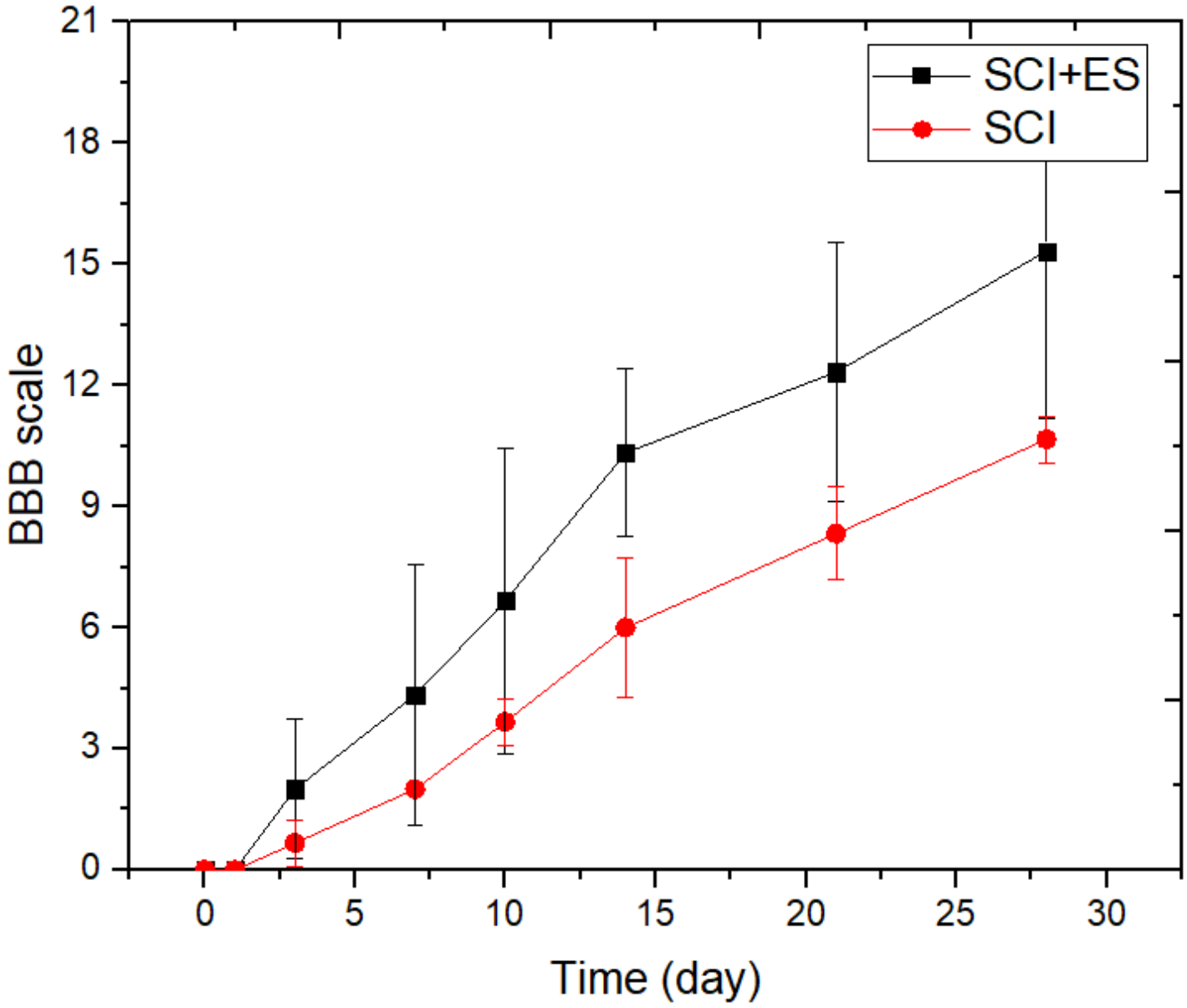

Figure 2

Comparison of BBB scores between SCI+ES and SCI rats

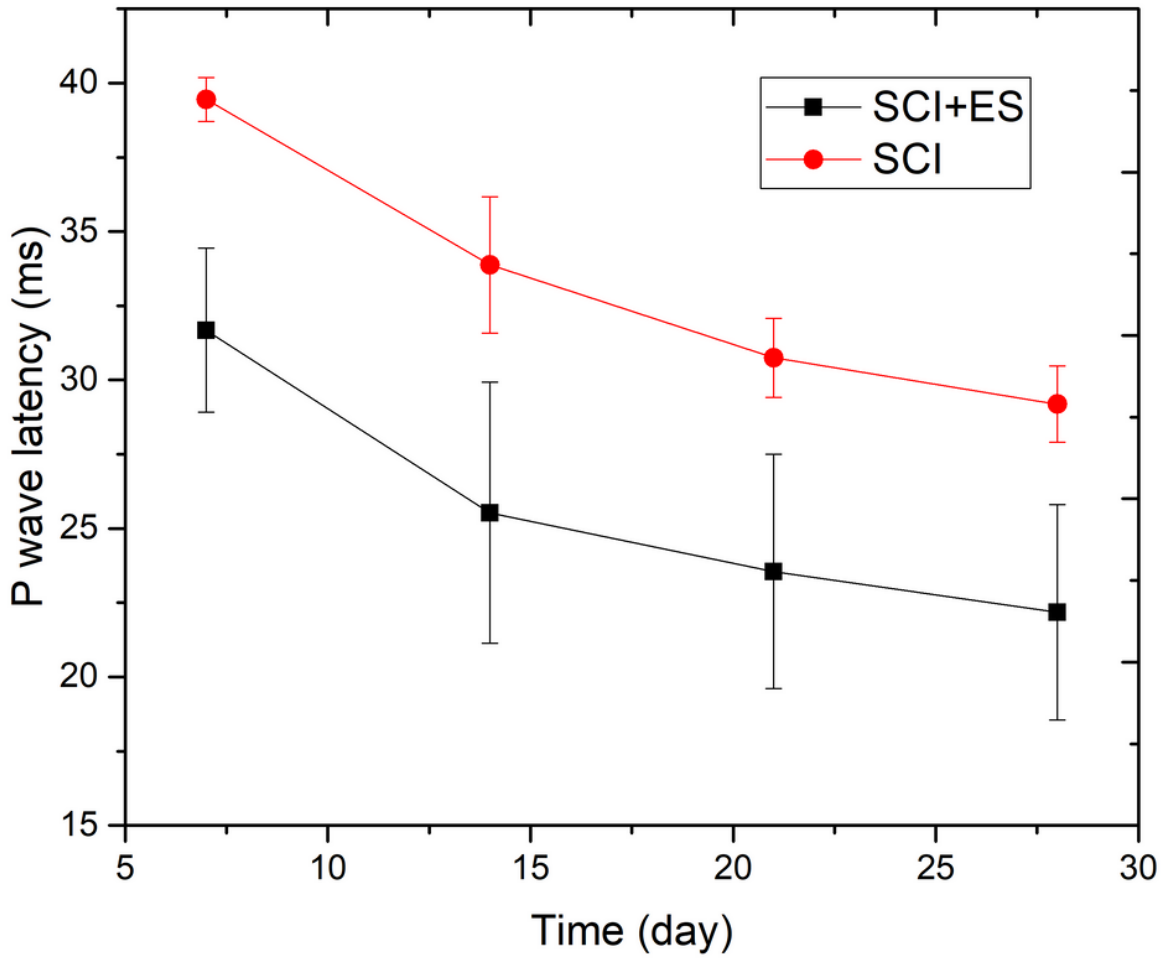

Figure 3

comparison of P wave latencies in SCI + ES, SCI and intact rats

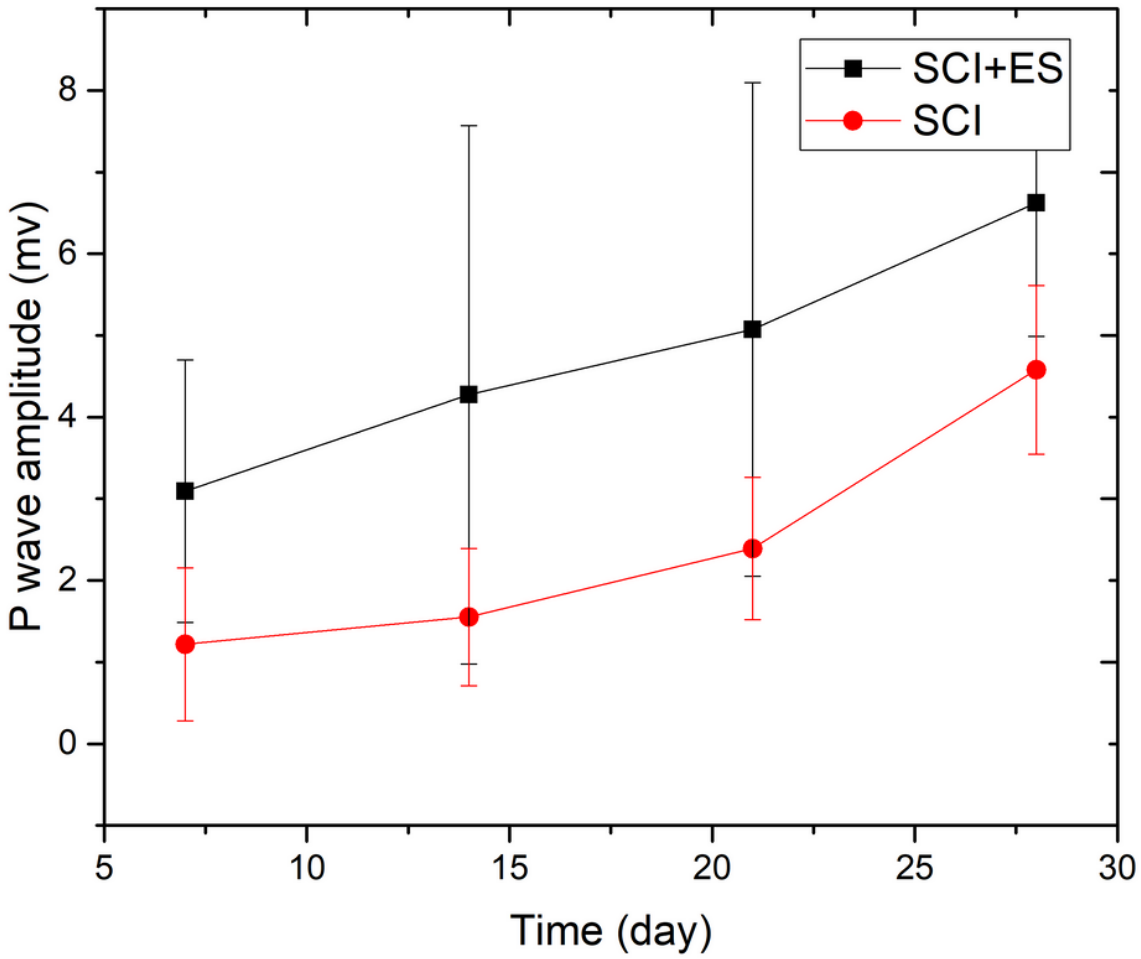

Figure 4

comparison of n wave latencies in SCI + ES, SCI and intact rats

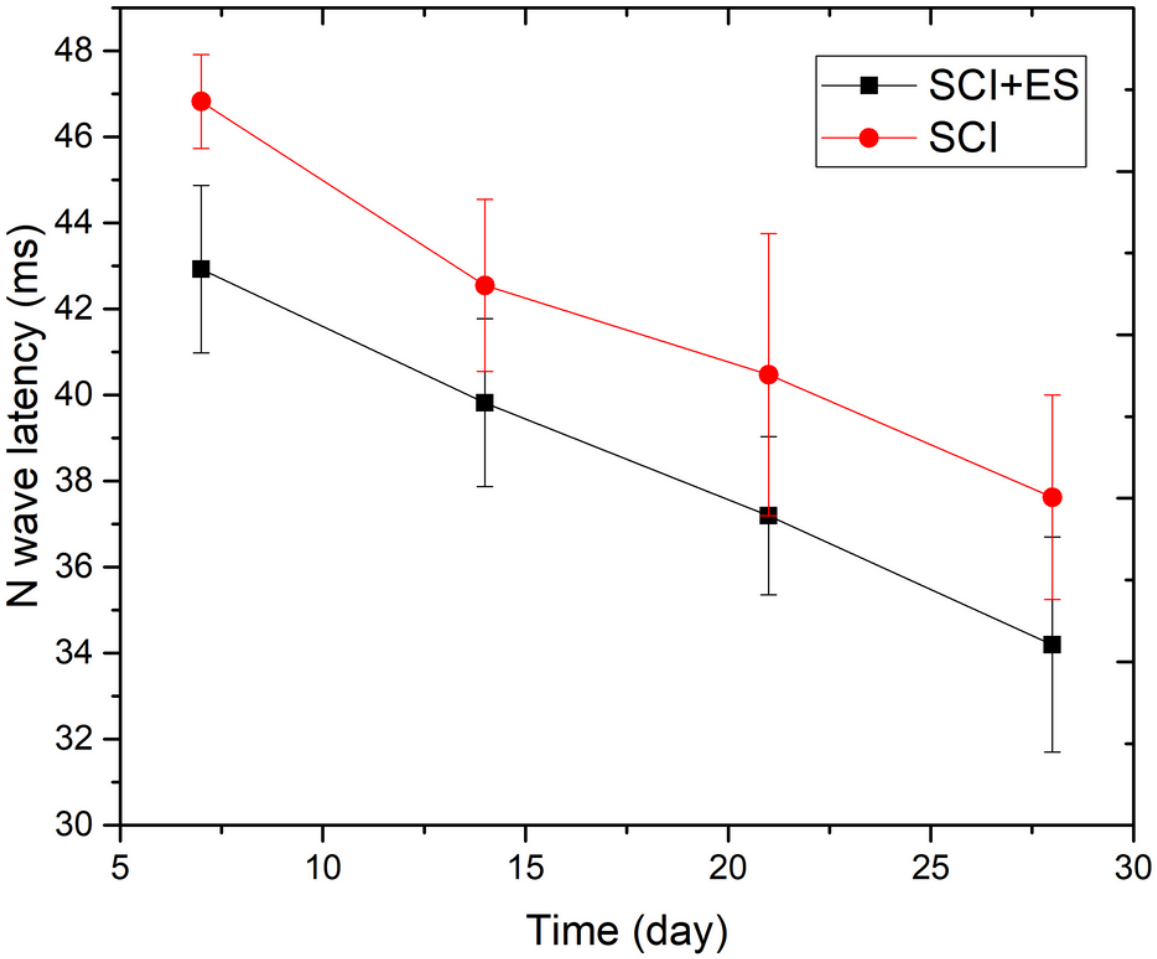

Figure 5

comparison of n wave latencies in SCI + ES, SCI and intact rats

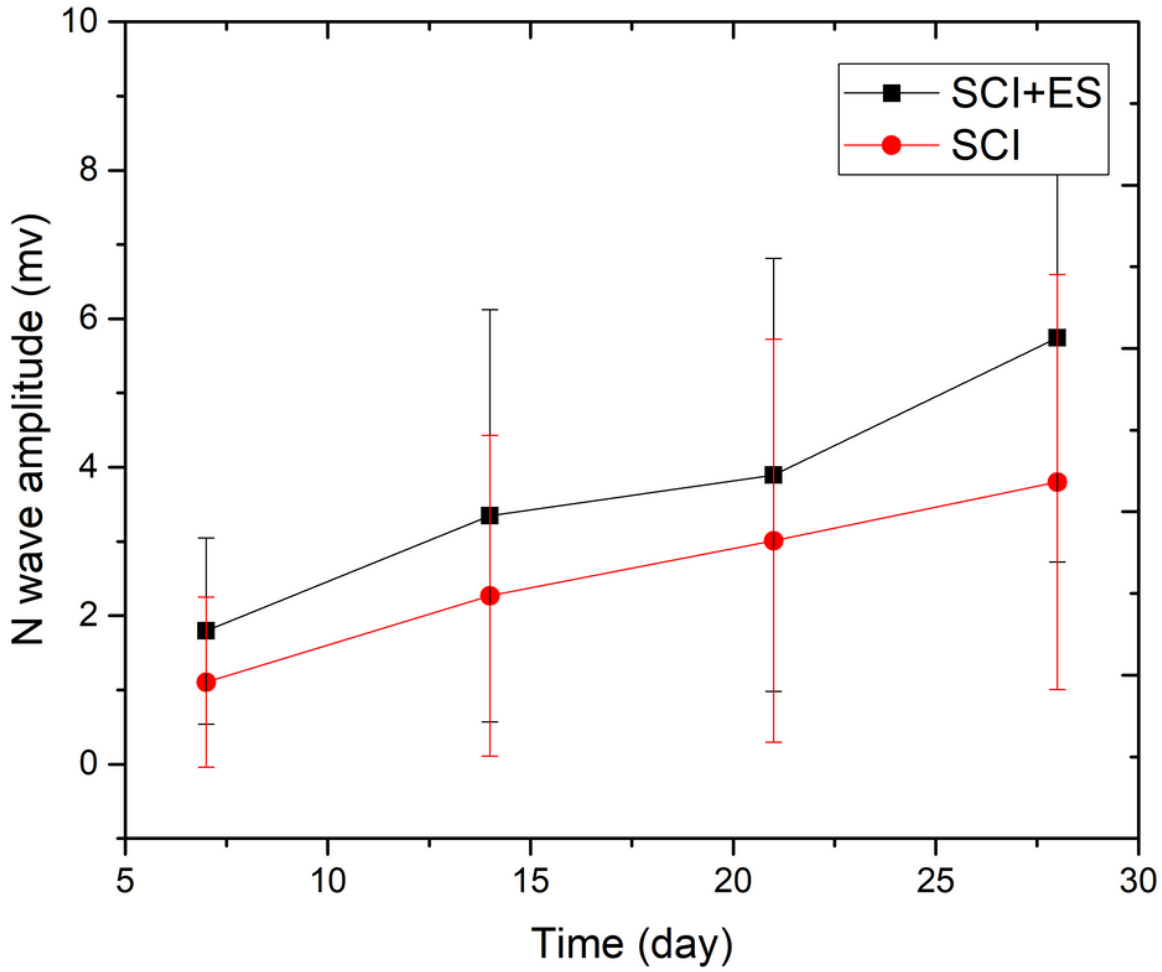

Figure 6

comparison of n wave amplitude of SCI + ES, SCI and intact rats

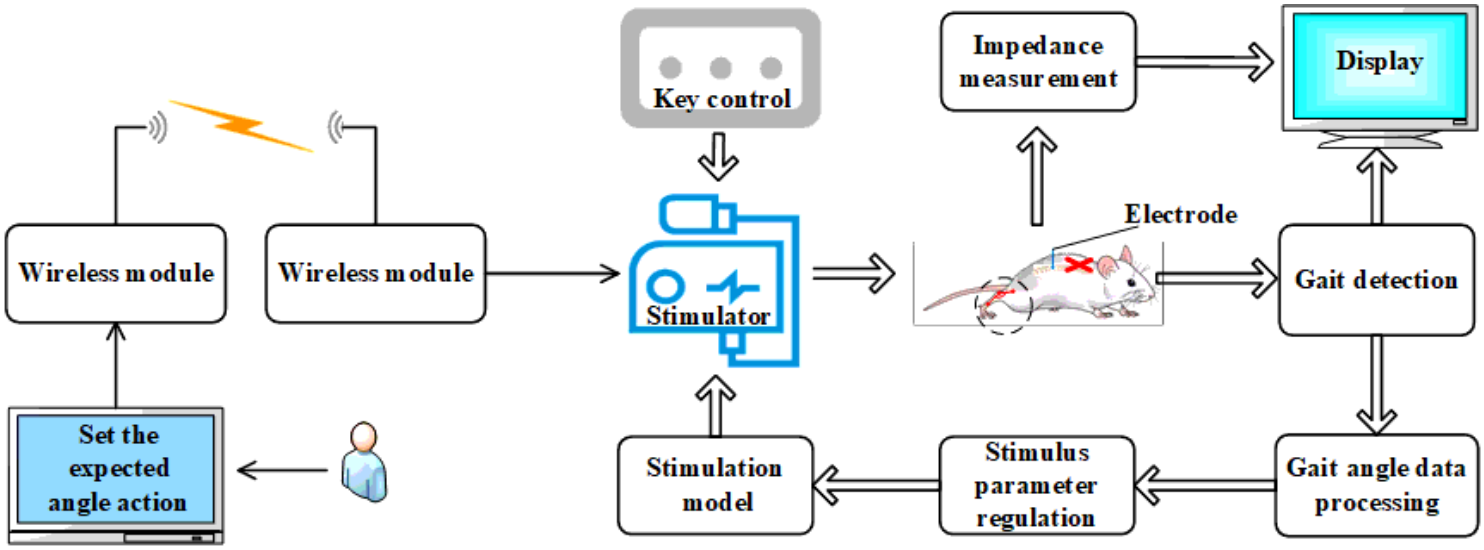

Figure 7

Overall block diagram of the system

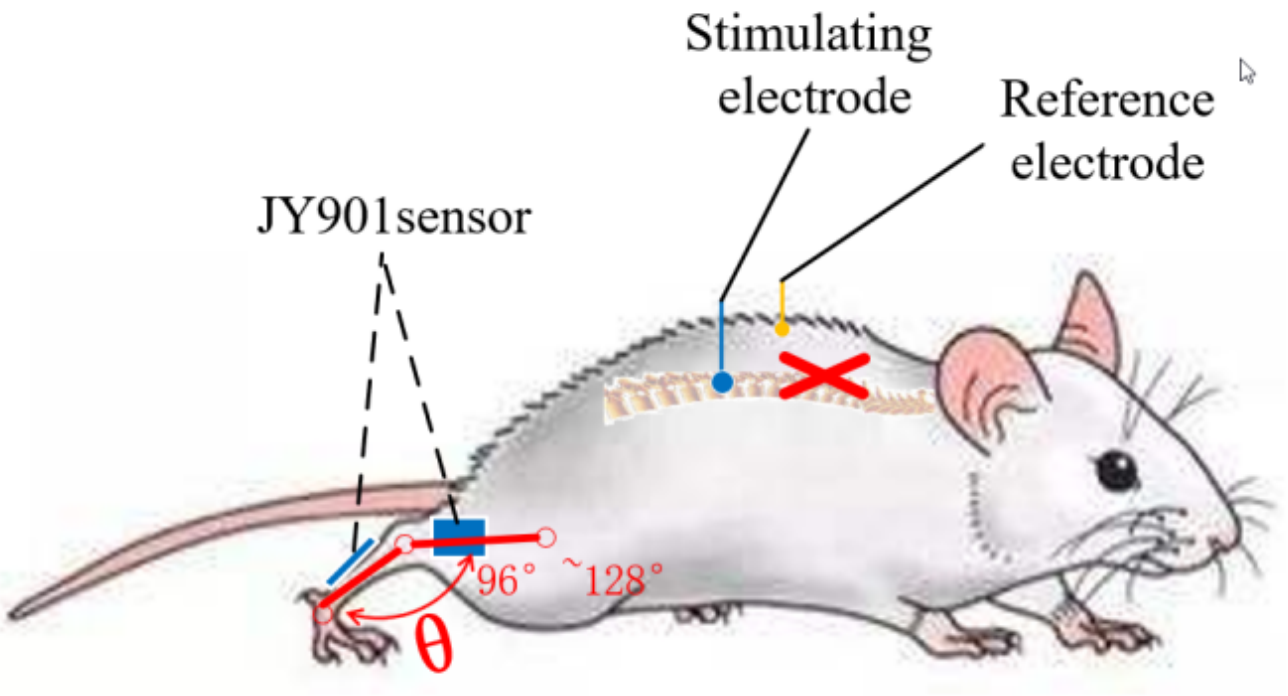

Figure 8

JY901 were located at the fixed position of rat hind limbs and knee joint angle θ

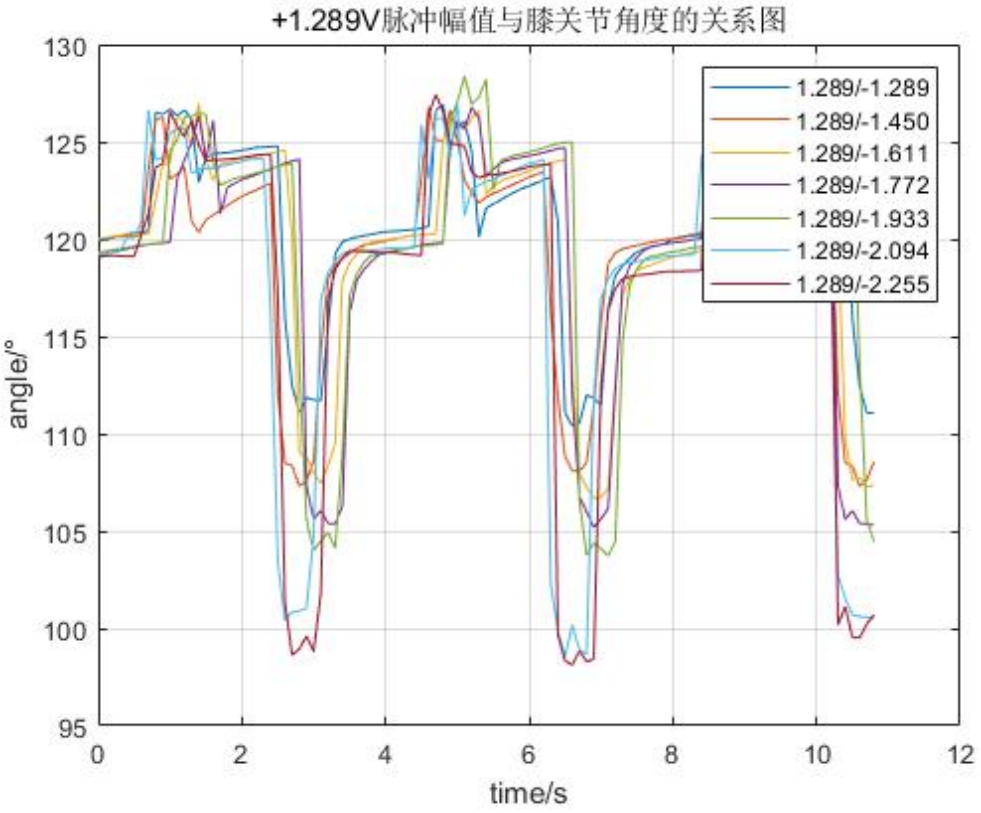

Figure 9

the positive pulse amplitude remains unchanged at 1.289v, and the negative voltage changes in the adjustable range

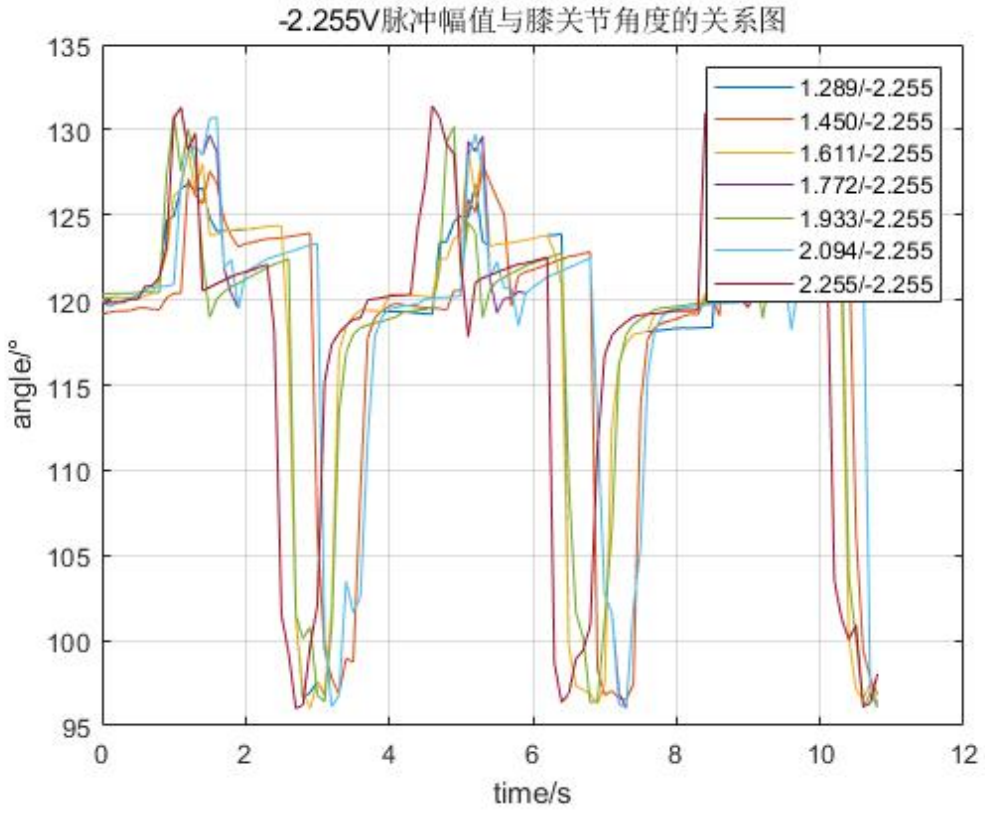

Figure 10

the amplitude of negative pulse remains unchanged at minus 2.255v, and the positive voltage changes in an adjustable range

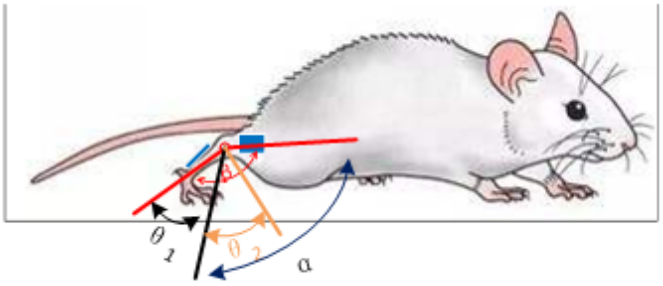

Figure 11

angles of hindlimbs of rats

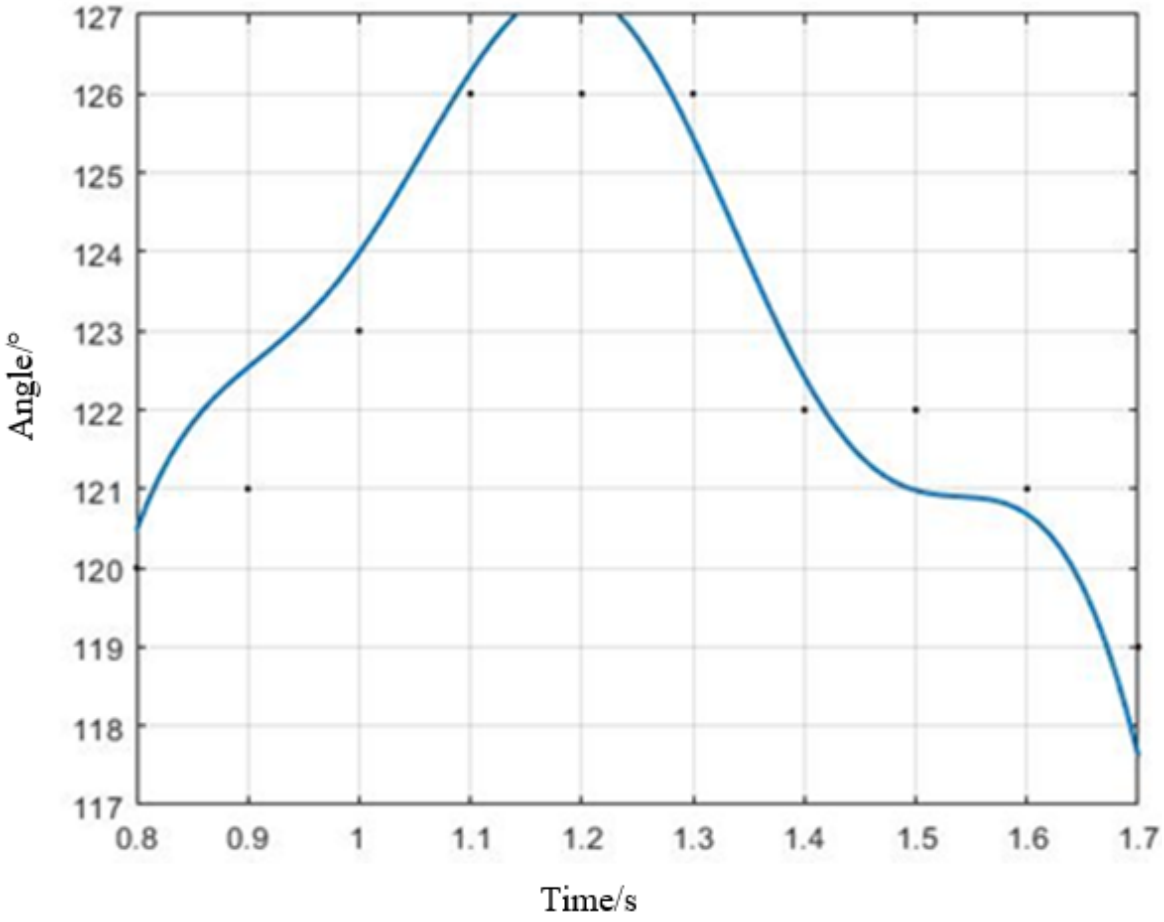

Figure 12

Positive pulse reference frame

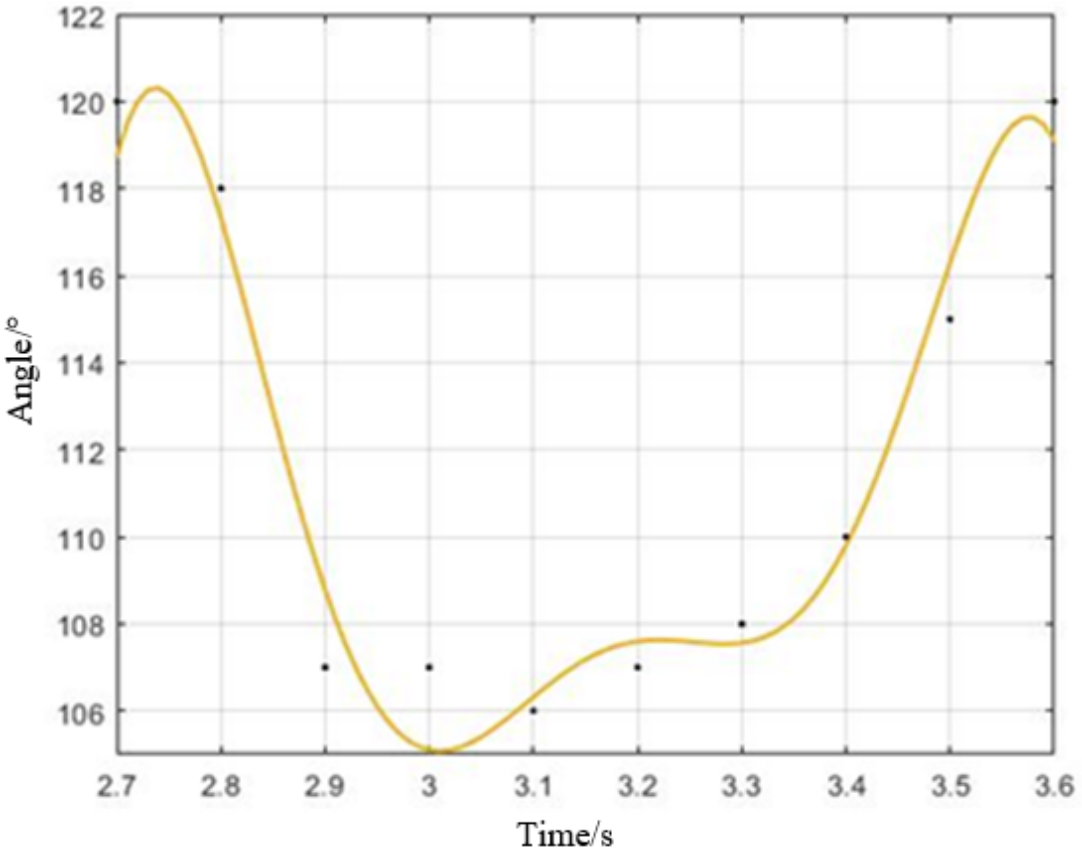

Figure 13

Negative pulse reference frame

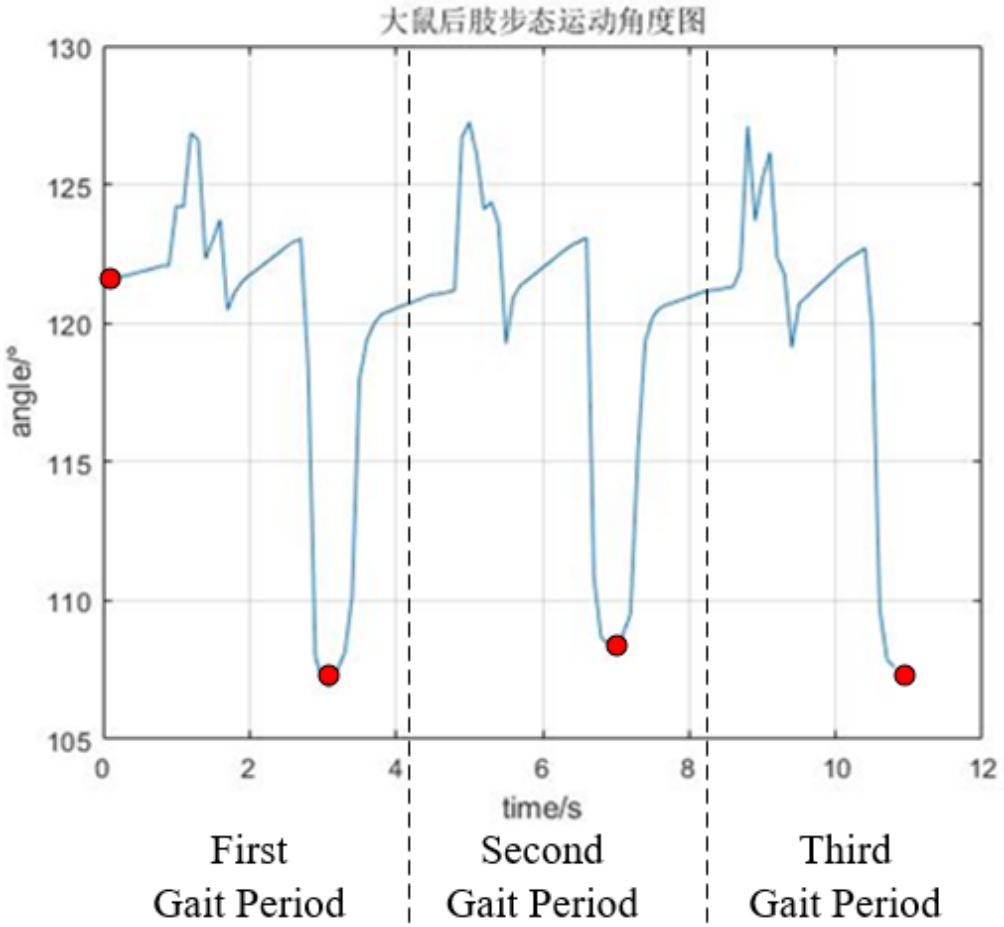

Figure 14

Gait cycle and calibration point (red is calibration point)

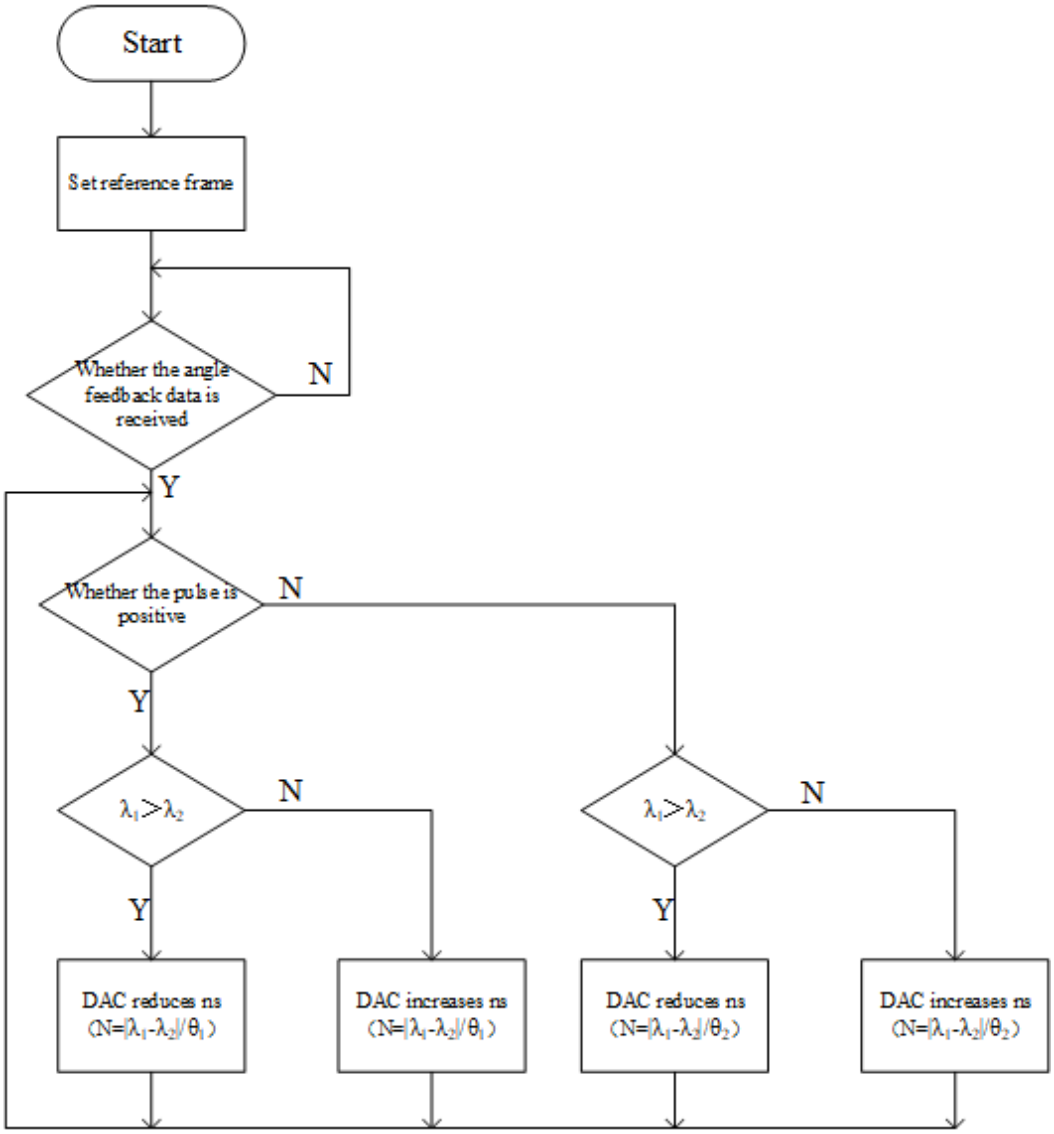

Figure 15

Flow chart of closed-loop control algorithm